Chemical Physics Letters 678 (2017) 79–84

Contents lists available at ScienceDirect

Chemical Physics Letters

journal homepage: www.elsevier.com/locate/cplett

Research paper

# Effect of $C_{60}$ adducts on the dynamic structure of aromatic solvation shells

James S. Peerless, G. Hunter Bowers, Albert L. Kwansa, Yaroslava G. Yingling *

*Department of Materials Science and Engineering, North Carolina State University, 911 Partners Way, Raleigh, NC 27695, United States*

ARTICLE INFO

*Article history:*
Received 17 December 2016
In final form 3 April 2017
Available online 5 April 2017

*Keywords:*
Fullerenes
Solubility
Molecular dynamics simulations
Structure analysis

ABSTRACT

We report herein on the use of all-atom molecular dynamics simulations to investigate the solvation environment of $C_{60}$ and four $C_{60}$-derived fullerenes immersed in a variety of aromatic solvents. Utilizing a recently developed solvation shell analysis technique that quantifies the spatial relationships between fullerenes and solvent on a molecular level, we show that the number of fullerene substituents and solvent chemistry are crucial determinants of the solvation shell structure and thus fullerene solvation behavior. Specifically, it is shown for the derivatives investigated that the number of fullerene substituents is more critical to solvation behavior than the substituent chemistry.



## 1. Introduction

Since its discovery in 1985 by Kroto and colleagues [1], the properties and applications of $C_{60}$ fullerene have been an active area of research due to the unique properties and chemical interactions of the molecule. Among the most fascinating, and often baffling, aspects of fullerene chemistry has been the behavior of $C_{60}$ in solvents [2–7]. Simultaneously, the exceptional ability of $C_{60}$ fullerene to accept and conduct electrons in all-organic electronics has made $C_{60}$ an early candidate as an electron acceptor species in organic photovoltaic (OPV) devices [8]. The interplay between these two properties – solubility and electronic properties – has proven crucial to OPV device performance [9,10]. Thus, efforts to improve either solubility, charge transfer, or both have led to the synthesis of a variety of fullerene derivatives for OPV applications [11,12].

The most ubiquitous of these fullerene derivatives, so much so that it is commonly regarded as the benchmark acceptor material for fullerene-polymer OPVs, is phenyl-$C_{61}$-butyric acid methyl ester (PCBM) [13,14]. The adduct unit of PCBM dramatically improves solubility over that of $C_{60}$ while maintaining electronic properties. Although PCBM use is widespread, there is a theoretical limit to device open circuit voltage ($V_{OC}$) based on the lowest unoccupied molecular orbital (LUMO) of PCBM [15,16]. Hence, researchers have synthesized and tested other fullerene additives, such as the bisadduct analog of PCBM, bisPCBM [17], and the mono- and bisadduct versions of the indene-modified fullerene, indene-$C_{60}$ monoadduct (ICMA) and indene-$C_{60}$ bisadduct (ICBA) [16]. Structures of these fullerene derivatives are shown below in Fig. 1.

The solubility of these materials is critical, not only to their ability to be processed during the liquid-phase deposition of these materials, but also to ultimate device performance [10]. For example, the higher LUMO level of bisPCBM should translate to a higher-efficiency device compared to those fabricated with PCBM, yet such a performance improvement is not observed presumably due to the poor miscibility of bisPCBM with polymer donor materials [18]. Moreover, the measurement of miscibility and solubility properties of fullerene derivatives is non-trivial given their low solubility and proclivity to exist as metastable solvates and crystalline phases in solvent [5,19].

Molecular dynamics (MD) is one of the best techniques to investigate the nanoscale solvation of fullerene materials as it can provide qualitative and quantitative insight into solvent environments at atomistic resolution. As a result, several recent studies have employed MD to investigate the behavior of fullerenes in solvent [20–30]. In particular, MD simulations were used to describe the solvation of fullerenes in aromatic solvents by analyzing the solvation shell of solvent immediately surrounding the fullerene cage [20–23]. For example, Wang et al. investigated the dynamic and static properties of the solvation shell around both $C_{60}$ and PCBM in five solvents using a coarse-grained united-atom MD method [21]. We recently employed all-atom MD techniques to observe and describe the formation of the solvation shell structure around $C_{60}$ and PCBM in nine aromatic solvents in comparison with experimentally measured solubility [20].

* Corresponding author.
*E-mail address:* yara_yingling@ncsu.edu (Y.G. Yingling).

http://dx.doi.org/10.1016/j.cplett.2017.04.010
0009-2614/

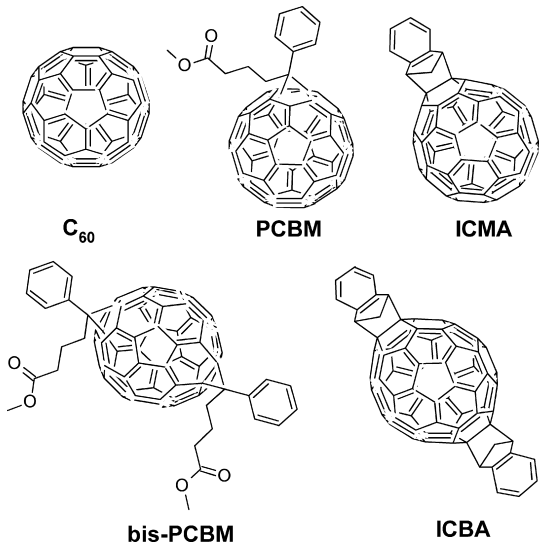


**Fig. 1.** Structures of $C_{60}$ fullerene and fullerene derivatives used in this study.

In this work, we apply an all-atom MD simulation technique to fullerene-solvent systems to better describe the nature of the solvation shell and elucidate details of fullerene solvation in aromatic solvents. Five fullerene species ($C_{60}$, PCBM, bisPCBM, ICMA, and ICBA) were used to understand the role of fullerene adduct chemistry (e.g., PCBM vs. ICMA) and substituent quantity (e.g., PCBM vs. bisPCBM) on solvation properties. These fullerenes were solvated in nine aromatic solvents (see Table 1) to investigate a variety of substitutional chemistries and positions. Utilizing both static and dynamic analysis, we attempt to correlate solvation environment to fullerene and solvent chemistry.

## 2. Methods

### 2.1. Simulation methods

All-atom MD simulations were performed with the AMBER 14 molecular dynamics package [31]. Atom types and corresponding force field parameters were assigned according to the general AMBER force field (GAFF) [32] with the exception of fullerene cage atoms. For $C_{60}$, non-bonded Lennard-Jones (LJ) parameters were modified to match those developed by Girifalco [33,34]. Validations of these parameters in comparison to other LJ parameters, such as those of the GAFF "*ca*" atom type (based on an aromatic carbon in benzene), for use in $C_{60}$ atomistic simulations have been performed elsewhere [20,29]. These Girifalco LJ parameters were also applied to the unmodified fullerene cage atoms (i.e., carbon atoms of the fullerene cage not bonded to any substituent atoms) of PCBM, bisPCBM, ICMA, and ICBA. All other atoms in the fullerene derivatives were assigned parameters according to GAFF. All partial charges were determined by the semi-empirical quantum mechanical AM1-BCC method [35,36].

**Table 1**
List of solvents under study and their abbreviations.

| Solvent | Abbreviation |
|---|---|
| 1,2,4-Trichlorobenzene | aTCB |
| 1,2,4-Trimethylbenzene | aTMB |
| Bromobenzene | BB |
| Benzene | Benz |
| Chlorobenzene | CB |
| 1,2-Dichlorobenzene | ODCB |
| *o*-Xylene | oX |
| Styrene | Styr |
| Toluene | Tol |

Fullerene-solvent systems consisted of a single fullerene in a periodic box of solvent large enough such that the fullerene would not interact with periodic images of itself (i.e., infinite dilution). Data was collected from 60-ns constant number-of-particles/pressure/temperature (NPT) simulations at 1 atm and 300 K. Data on solvent-only systems (≈790,000 Å$^3$ periodic boxes) was collected from 10-ns NPT simulations at 1 atm and 300 K. In total, data was collected from 54 independent simulations (9 solvents × (5 fullerenes + 1 solvent-only)). Details on the volume and number of atoms for each simulation are provided in the Supplemental Information (SI, see Section S1). Also included in the SI is a description of the system equilibration procedure performed prior to data-collection steps (see Section S1).

### 2.2. Analysis methods

Raw data, such as interatomic distances and angles, were extracted from MD trajectories with AMBER's post-processing tools [37] and the MDAnalysis Python package [38]. The data were further analyzed using in-house programs to produce the two primary solvation shell analytical parameters reported herein, namely, the degree of order (DoO) [20] and the occupational time correlation function (OTCF).

We recently developed a method that permits assessment of the solvation shell DoO, a quantification of solvation shell structural regularity (propensity of solvent molecules to assume a singular orientation and distance around a solute), which has been reported in detail elsewhere [20]. In brief, the method takes the distance between the center of mass (CoM) of the fullerene cage to the CoM of the aromatic carbons on the solvent molecule ($d$) and the angle between the fullerene cage CoM, the solvent aromatic carbon CoM, and a solvent indicator atom (typically representing the location of a substituent) ($\theta$) for each solvent molecule at each timestep (see Fig. 2). These $d$-$\theta$ data are then processed through a 2-dimensional histogram binning process to provide a relative frequency for each $d$-$\theta$ bin. (This histogram data can be conveniently visualized as a contour plot, which is provided in the SI for each fullerene-solvent system; see Section S2.) The DoO is computed from a scanning algorithm that calculates the number of $d$-$\theta$ points at the most frequent $d$-$\theta$ region in terms of a percentage of all the $d$-$\theta$ data points found in the solvation shell throughout the trajectory.

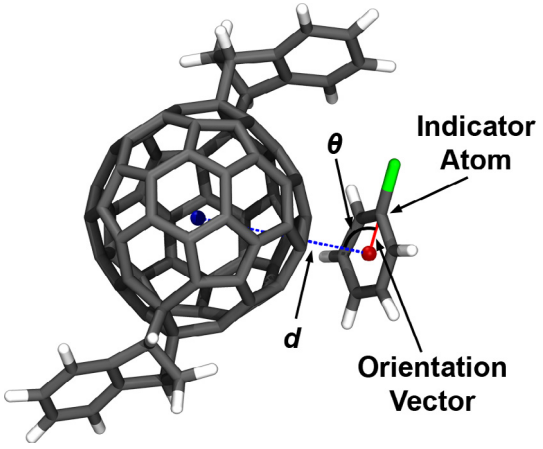


**Fig. 2.** Diagram of ICBA and a molecule of CB illustrating distance vector ($d$) and orientation angle ($\theta$) used to calculate degree of order (DoO).

The OTCF is a temporal function commonly used to describe the frequency with which a solvent molecule will leave a particular area and has commonly been applied to MD simulations of solvated systems [39], including those containing fullerenes [21,22]. The OTCF ($R(t)$) is calculated as follows:

$$R(t) = \frac{\left\langle \sum_{i=1}^{N} \theta_i(t_0)\theta_i(t+t_0) \right\rangle}{\left\langle \sum_{i=1}^{N} \theta_i(t_0)\theta_i(t_0) \right\rangle}, \quad \theta_i = \begin{cases} 1, & r \leqslant r_c \\ 0, & r > r_c \end{cases}$$

where $N$ is the total number of solvent molecules, $t_0$ is the time origin, $t$ is the current simulation time, $r$ is the distance between solvent CoM and solute CoM, $r_c$ is the critical distance, and angle brackets ($\diamond$) denote an ensemble average based on multiple time origins. For fullerene-solvent systems, $r_c$ represents the radius of the solvation shell, which is determined to be 10 Å via examination of solvent radial distribution function (RDF) data obtained from simulations (see SI, Section S3). This value of 10 Å is also used as the solvation shell limit for DoO calculations. For solvent-only systems, $r_c$ was set to 9 Å to approximate the same volume as a 10-Å sphere minus the volume of a $C_{60}$ molecule.

## 3. Results and discussion

In our previous work [20], we showed that DoO correlates to solubility only when systems containing the same fullerene are compared to one another. In Fig. 3, we plotted DoO values for all fullerene-solvent systems under study. If one considers each data series in Fig. 3 as a group, DoO values within that group are shown to correlate with solubility in the case of $C_{60}$ and PCBM. This correlation has not been shown to hold when comparing values between groups. For example, the DoO of $C_{60}$ in CB is higher than that of PCBM in CB even though PCBM is more soluble in CB than $C_{60}$ in CB. Thus, only DoO comparisons between systems containing the same fullerene are valid for extrapolating trends in solubility.

With this in mind, we note that in the absence of experimental solubility limits for a large number of the systems investigated in this study, there is not enough data to convincingly reproduce the correlation of DoO to solubility limits for bisPCBM, ICMA, and ICBA. We have included a discussion of DoO as a function of Hansen solubility parameters (HSPs), often used to qualitatively predict solubility, in the SI (see Section S4). No correlation is apparent (see Fig. S7), yet the HSP distances ($R_a$) are not particularly well-suited for predicting solubility for these systems ($C_{60}$ fullerenes in aromatic solvent). This may be due to a variety of reasons including similar HSPs for the solvents investigated, metastable solvate formation, low solubility limits, etc. In the interest of space, readers are referred to the following sources for a more detailed discussion of the use of HSPs and other solvent descriptors for fullerene solvation [5,30,40].

Based on the previous results of DoO for $C_{60}$- and PCBM-containing systems, it is reasonable to assume that DoO also has an effect on solvation behavior for the remaining fullerene derivatives (bisPCBM, ICMA, ICBA). Thus, trends in DoO data from each fullerene data set in Fig. 3 can be examined to highlight changes in solvation shell structure due to the presence of different adducts. Fig. 3 shows that the DoO trends of monoadducts (PCBM and ICMA) and bisadducts (bisPCBM and ICBA) more closely mimic each other than those of derivatives with the same adduct chemistry (PCBM and bisPCBM, for example). This suggests that the number of substituents present on a fullerene derivative may be more influential to solvation behavior than the chemistry of the adduct itself. Upon further inspection, the deviations between bisadduct and monoadduct fullerenes are most pronounced in the case of solvents aTCB, aTMB, and ODCB. These three solvents, along with *o*-xylene, have more than one substituted unit on the benzene ring.

The OTCF data can be used to gain further context for the dynamic nature of the solvation shell. The solvent half-life ($t_{1/2}$) can be calculated from a two-term exponential fit to the OTCF $R(t)$ data for each fullerene-solvent and solvent-only simulation seen in Section S5 of the SI. This half-life, which is simply the time $t$ at which $R(t) = 0.5$, represents the dynamic stability of the solvation shell. Similar to DoO, it has been correlated with material solubility for both $C_{60}$ and PCBM by Wang and Hua [21]. The solvent half-life data calculated from simulations performed for this study are shown in Fig. 4.

The immediate comparison between DoO trends in Fig. 3 and the $t_{1/2}$ data in Fig. 4 is that the $t_{1/2}$ values do not deviate nearly as much from one fullerene to another. The trend in $t_{1/2}$ data is remarkably similar for each fullerene as well as for the solvent-only systems. Thus, the dynamic stability of the solvation shell is much more dependent on the solvent species than the nature of the fullerene derivative. However, it can also be noted that across all solvents, the bisadducts exhibit slightly higher $t_{1/2}$ values, followed by the monoadducts, and lastly by unmodified $C_{60}$. This somewhat unexpected result suggests that the steric hindrance

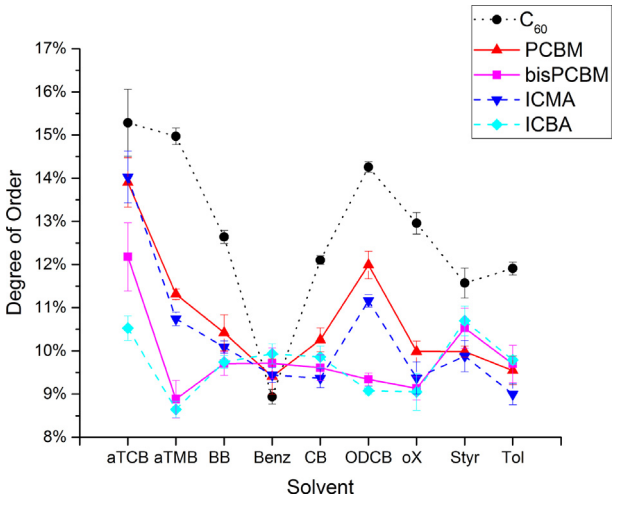


**Fig. 3.** Degree of order for each fullerene-solvent system.

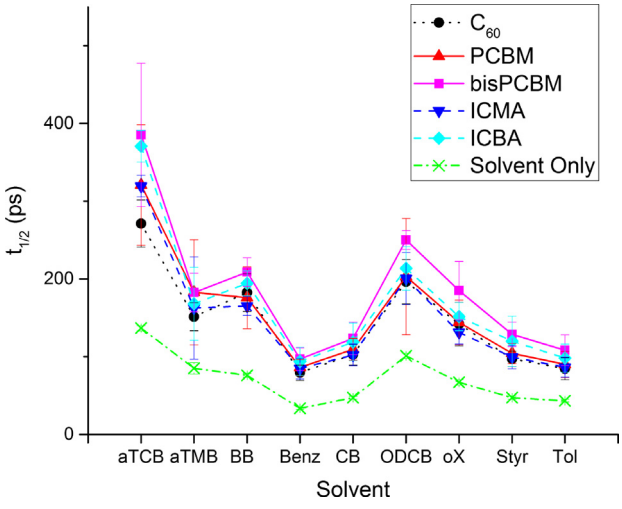


**Fig. 4.** Solvent half-life ($t_{1/2}$) calculated from fullerene-solvent and solvent-only simulations. See Fig. S6 in the SI for the complete OTCF $R(t)$ data.

introduced by the two adduct units has a stabilization effect on the solvation shell; the additional units on the fullerene appear to effectively trap solvent molecules inside the solvation shell for longer periods of time.

It should be noted that aTCB stands out as a significant high point in both DoO and $t_{1/2}$ data. This result can likely be attributed to the relatively high melting point of aTCB (290.5 K), which is the highest of the solvents investigated in this study. Thus, it is reasonable to assume that aTCB would display the highest degree of solvation shell order and the slowest movement in and out of the solvation shell at 300 K.

When comparing DoO and $t_{1/2}$ data across the investigated systems, the divergence in behavior among fullerene derivatives becomes apparent. Cursory visual inspection of the data in Figs. 3 and 4 suggests that some fullerene derivatives exhibit trends in DoO data that closely mimic $t_{1/2}$ data while others do not. A positive correlation between DoO and $t_{1/2}$ would be expected, as solvent molecules that display more orientational order (high DoO) are expected to be more dynamically stable (high $t_{1/2}$).

The correlation between DoO and $t_{1/2}$ data was explicitly investigated for each of the fullerene derivatives, and the associated correlation coefficients (R-values) were calculated (see Fig. 5). It is immediately obvious that the monoadducts (PCBM, Fig. 5b; ICMA, Fig. 5d) exhibit a strong positive correlation between DoO and $t_{1/2}$ data with R-values of 0.954 and 0.931 for PCBM and ICMA, respectively. $C_{60}$ (Fig. 5a) exhibits an R-value of 0.757, which is considerable but weak compared to that of the monoadducts. It should be noted that the major negative outlier in the $C_{60}$ correlation represents the benzene-$C_{60}$ system, which exhibits a lower-than-expected DoO value likely as a result of the symmetry of the solvent molecule [20]. For both bisadduct species, the DoO-$t_{1/2}$ correlation is extremely weak, exhibiting absolute R-values of 0.042 and 0.242 for bisPCBM (Fig. 5c) and ICBA (Fig. 5e), respectively. Moreover, contrary to what one would expect, both linear fits show a slight negative slope indicating a negative correlation between DoO and $t_{1/2}$. It should also be noted that for both the bisPCBM and ICBA correlations, the only systems that exhibit negative residuals (i.e., lie below the trend line in Fig. 5c and e) correspond to aTMB, ODCB, and oX. All of these solvents contain more than one substituted unit, along with aTCB which is consistently at the high end of both DoO and $t_{1/2}$ values.

The carbon atoms in the fullerene cage for all the fullerene species had identical van der Waals interaction parameters. Thus, a given solvent molecule will be equivalently attracted to the

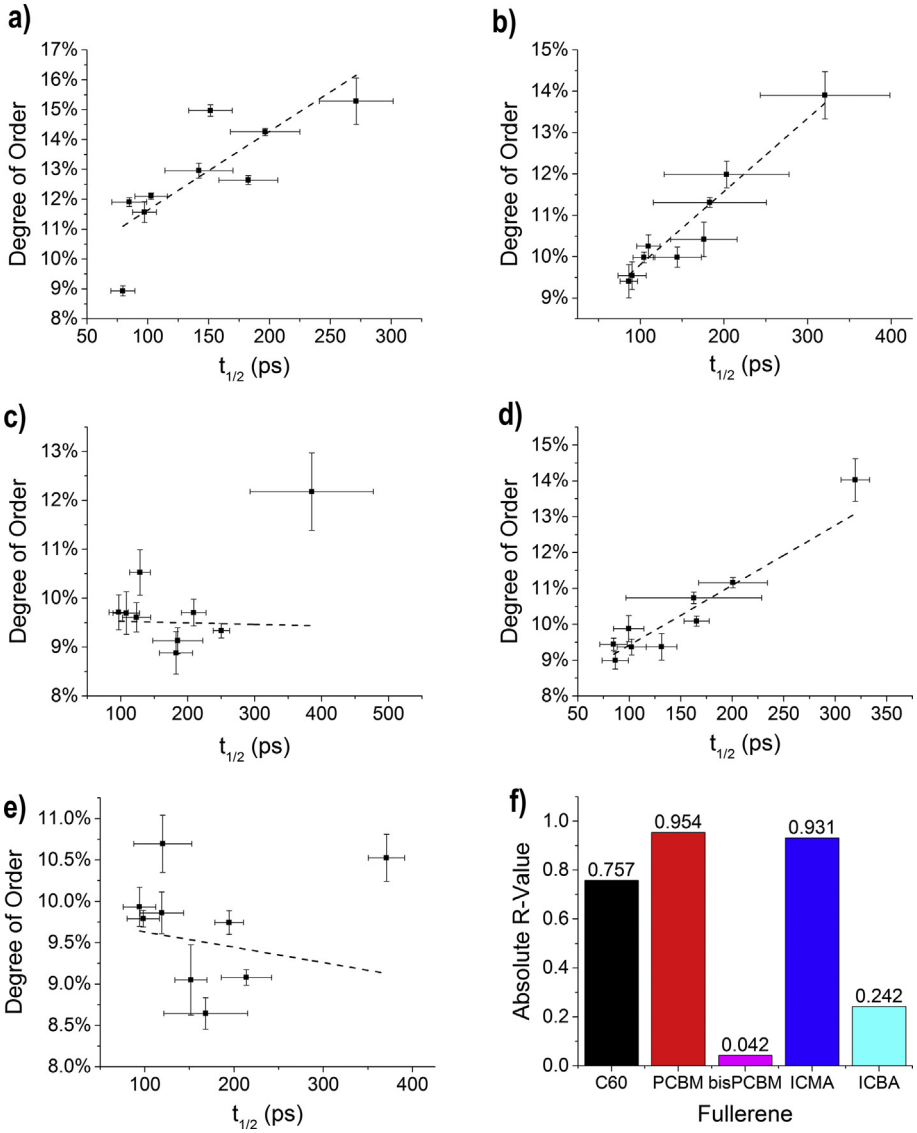


**Fig. 5.** Degree of order as a function of solvent half-life ($t_{1/2}$) for (*a*) $C_{60}$, (*b*) PCBM, (*c*) bisPCBM, (*d*) ICMA, (*e*) ICBA systems. (*f*) Absolute R-values of linear fits to data in *a*-*e*.

fullerene cage regardless of fullerene adduct chemistry, with the exception of minor differences in atomic partial charge parameters caused by electron-withdrawing groups present on the adduct (e.g., oxygen present in PCBM). With roughly equivalent solvent-cage interactions, the primary driving forces for the movement of solvent molecules in and out of the solvation shell (e.g., solvent-cage interaction energy and diffusivity) are similar between systems composed of the same solvent. Derivative-specific solvent-substituent interactions are not a strong factor in the movement of solvent molecules close to the fullerene cage. Given that the limits of the solvation shell in this experiment are measured from the center of the fullerene cage, most of the solvent molecules interacting primarily with the substituent unit are outside of the solvation shell. Thus, it stands to reason that all derivatives show equivalent trends in $t_{1/2}$ values.

Conversely, DoO values are much more dependent on the fullerene adduct. PCBM exhibits the strongest correlation between DoO and $t_{1/2}$ data, which is likely due to its adduct chemistry. The PCBM adduct, being composed of a flexible chain and freely-rotating phenyl group, is a much more flexible structure than that of ICMA. The bisadducts, for which such a correlation is practically nonexistent, possess an even higher barrier to direct solvent interactions with the fullerene cage atoms because of the two substituted groups. Although the ICBA data yields a higher absolute R-value than the bisPCBM data, it should be noted that the slope of the ICBA fit is more strongly negative. This may similarly be a result of the lower flexibility of indene groups in comparison to the PCBM substituent. Overall, the DoO clearly depends on the amount of unperturbed surface area of the fullerene cage around which a regular solvation shell can easily form.

An explanation of this DoO behavior in terms of solvent species is less straightforward. For example, there is no clear solvent property that separates solvents for which DoO values are roughly equivalent for PCBM and ICMA (benzene, styrene, and aTCB) and solvents for which ICMA DoO values are lower than PCBM DoO values (*o*-xylene, aTMB, toluene, chlorobenzene, ODCB, and bromobenzene). In the comparison between the bisadduct and monoadduct DoO behavior, it is noted above that the most drastic deviations are seen for aTMB, aTCB, and ODCB. These three solvents are tri- or di-substituted and thus exhibit relatively high molar volumes. It may be tempting to attribute the observed dramatic reduction in the degree of order to the larger volume of these solvent molecules relative to the other solvents in this study. Yet this line of thinking begs the question of why such a dramatic effect is not observed for *o*-xylene, which is also di-substituted with relatively bulky methyl groups. Interestingly, *o*-xylene does show up, along with aTMB and ODCB, as one of the few solvents that exhibits negative residuals to the weak DoO-$t_{1/2}$ correlations for bisadduct systems, suggesting that *o*-xylene may also produce suppressed DoO values for bisadducts.

## 4. Conclusions

We report on the properties of the solvation shell as observed by MD simulations for systems composed of $C_{60}$ and four $C_{60}$ derivatives in nine aromatic solvents. From these simulations, we calculate both a dynamic property (solvent half-life, $t_{1/2}$) and a structural descriptor (degree of order, DoO).

These data ($t_{1/2}$ and DoO) produced intriguingly divergent results. Trends in the $t_{1/2}$ data were much more consistent between fullerene derivatives. Conversely, DoO data shows significant variation between fullerene species. Most notably, fullerene derivatives that have the same number of adducts show more similar DoO trends than a monoadduct and bisadduct with the same adduct chemistry. Thus it is suggested that the number of fullerene substituents is more critical to solvation behavior than the adduct species itself for the derivatives investigated.

DoO data from PCBM, which possesses a single flexible adduct, exhibits the strongest correlation with $t_{1/2}$ values. ICMA shows similar behavior with minor deviations that may be attributed to the lower flexibility of its adduct species. Further, extremely weak DoO-$t_{1/2}$ correlations measured in bisadduct systems are likely attributed to increased steric hindrance and decreased cage surface area.

The data reported herein represents physical insights into the solvation environment only attainable by nanoscale simulation methods. The results not only serve to inform experimentalists of the complex underlying processes of solvation for these unique fullerene materials, but also put forth useful methodology to describe solvation environments that may be applied to a broad range of molecular and colloidal materials. It is hoped that the recognition of dynamic structures present in organic solvents may be further investigated for anomalous solvation behavior observed macroscopically in a broad range of solutes.

## Acknowledgement

This work was partially supported by the National Science Foundation Research Triangle MRSEC (DMR-1121107) and the NSF Research Traineeship on Data-Enabled Science and Engineering of Atomic Structure (DGE-1633587). Computational resources were partially provided by the High Performance Computing Center at North Carolina State University.

## Appendix A. Supplementary data

Supplementary data associated with this article can be found, in the online version, at http://dx.doi.org/10.1016/j.cplett.2017.04.010.

## References

[1] H.W. Kroto, J.R. Heath, S.C. Obrien, R.F. Curl, R.E. Smalley, C-60 - buckminsterfullerene, Nature 318 (1985) 162–163.
[2] R.S. Ruoff, R. Malhotra, D.L. Huestis, D.S. Tse, D.C. Lorents, Anomalous solubility behavior of C60, Nature 362 (1993) 140–141.
[3] G. Andrievsky, V. Klochkov, E. Karyakina, N. Mchedlov-Petrossyan, Studies of aqueous colloidal solutions of fullerene C-60 by electron microscopy, Chem. Phys. Lett. 300 (1999) 392–396.
[4] N.O. Mchedlov-Petrossyan, Fullerenes in molecular liquids. Solutions in "good" solvents: another view, J. Mol. Liq. 161 (2011) 1–12.
[5] N.O. Mchedlov-Petrossyan, Fullerenes in liquid media: an unsettling intrusion into the solution chemistry, Chem. Rev. 113 (2013) 5149–5193.
[6] V.L.V. Chaban, C. Maciel, E.E. Fileti, Solvent polarity considerations are unable to describe fullerene solvation behavior, J. Phys. Chem. B 118 (2014) 3378–3384.
[7] N.O. Mchedlov-Petrossyan, N.N. Kamneva, Y.T.M. Al-Shuuchi, A.I. Marynin, S.V. Shekhovtsov, The peculiar behavior of fullerene C-60 in mixtures of 'good' and polar solvents: colloidal particles in the toluene-methanol mixtures and some other systems, Colloids Surf. A-Physicochem. Eng. Aspects 509 (2016) 631–637.
[8] N. Sariciftci, L. Smilowitz, A. Heeger, F. Wudl, Photoinduced electron-transfer from a conducting polymer to buckminsterfullerene, Science 258 (1992) 1474–1476.
[9] P.A. Troshin, H. Hoppe, J. Renz, M. Egginger, J.Y. Mayorova, A.E. Goryochev, et al., Material solubility-photovoltaic performance relationship in the design of novel fullerene derivatives for bulk heterojunction solar cells, Adv. Func. Mater. 19 (2009) 779–788.
[10] D.K. Susarova, A.E. Goryachev, D.V. Novikov, N.N. Dremova, S.M. Peregudova, V.F. Razumov, et al., Material solubility effects in bulk heterojunction solar cells based on the bis-cyclopropane fullerene adducts and P3HT, Sol. Energy Mater. Sol. Cells 120 (2014) 30–36.
[11] Y. He, Y. Li, Fullerene derivative acceptors for high performance polymer solar cells, Phys. Chem. Chem. Phys. 13 (2011) 1970–1983.
[12] C. Li, H. Yip, A.K.-.. Jen, Functional fullerenes for organic photovoltaics, J. Mater. Chem. 22 (2012) 4161–4177.
[13] G. Dennler, M.C. Scharber, C.J. Brabec, Polymer-fullerene bulk-heterojunction solar cells, Adv. Mater. 21 (2009) 1323–1338.

[14] K.A. Mazzio, C.K. Luscombe, The future of organic photovoltaics, Chem. Soc. Rev. 44 (2015) 78–90.
[15] M. Scharber, D. Wuhlbacher, M. Koppe, P. Denk, C. Waldauf, A. Heeger, et al., Design rules for donors in bulk-heterojunction solar cells - towards 10 % energy-conversion efficiency, Adv. Mater. 18 (2006) 789, 789-+.
[16] Y. He, H. Chen, J. Hou, Y. Li, Indene-C-60 bisadduct: a new acceptor for high-performance polymer solar cells, J. Am. Chem. Soc. 132 (2010) 1377–1382.
[17] M. Lenes, G.A.H. Wetzelaer, F.B. Kooistra, S.C. Veenstra, J.C. Hummelen, P.W.M. Blom, Fullerene bisadducts for enhanced open-circuit voltages and efficiencies in polymer solar cells, Adv. Mater. 20 (2008) 2116, 2116-+.
[18] M.A. Faist, S. Shoaee, S. Tuladhar, G.F.A. Dibb, S. Foster, W. Gong, et al., Understanding the reduced efficiencies of organic solar cells employing fullerene multiadducts as acceptors, Adv. Energy Mater. 3 (2013) 744–752.
[19] Y. Marcus, A. Smith, M. Korobov, A. Mirakyan, N. Avramenko, E. Stukalin, Solubility of C-60 fullerene, J. Phys. Chem. B 105 (2001) 2499–2506.
[20] J.S. Peerless, G.H. Bowers, A.L. Kwansa, Y.G. Yingling, Fullerenes in aromatic solvents: correlation between solvation-shell structure, solvate formation, and solubility, J. Phys. Chem. B 119 (2015) 15344–15352.
[21] C.I. Wang, C.C. Hua, Solubility of C60 and PCBM in organic solvents, J. Phys. Chem. B 119 (2015) 14496–14504.
[22] C.I. Wang, C.C. Hua, S.A. Chen, Dynamic solvation shell and solubility of C-60 in organic solvents, J. Phys. Chem. B 118 (2014) 9964–9973.
[23] S. Fritsch, C. Junghans, K. Kremer, Structure formation of toluene around C60: implementation of the adaptive resolution scheme (AdResS) into GROMACS, J. Chem. Theory Comput. 8 (2012) 398–403.
[24] S.R. Varanasi, O.A. Guskova, A. John, J. Sommer, Water around fullerene shape amphiphiles: a molecular dynamics simulation study of hydrophobic hydration, J. Chem. Phys. 142 (2015) 224308.
[25] J.I. Choi, S.D. Snow, J. Kim, S.S. Jang, Interaction of C-60 with water: first-principles modeling and environmental implications, Environ. Sci. Technol. 49 (2015) 1529–1536.
[26] V.V. Chaban, C. Maciel, E.E. Fileti, Does the like dissolves like rule hold for fullerene and ionic liquids?, J Solution Chem. 43 (2014) 1019–1031.
[27] S. Banerjee, Molecular dynamics study of self-agglomeration of charged fullerenes in solvents, J. Chem. Phys. 138 (2013) 044318.
[28] S.M. Mortuza, S. Banerjee, Molecular modeling study of agglomeration of [6,6]-phenyl-C61-butyric acid methyl ester in solvents, J. Chem. Phys. 137 (2012) 244308.
[29] L. Monticelli, On atomistic and coarse-grained models for C-60 fullerene, J. Chem. Theory Comput. 8 (2012) 1370–1378.
[30] J.D. Perea, S. Langner, M. Salvador, J. Kontos, G. Jarvas, F. Winkler, et al., Combined computational approach based on density functional theory and artificial neural networks for predicting the solubility parameters of fullerenes, J. Phys. Chem. B 120 (2016) 4431–4438.
[31] D.A. Case, V. Babin, J.T. Berryman, R.M. Betz, Q. Cai, D.S. Cerutti, et al., AMBER 14 (2014).
[32] J. Wang, R.M. Wolf, J.W. Caldwell, P.A. Kollman, D.A. Case, Development and testing of a general AMBER force field, J. Comput. Chem. 25 (2004) 1157–1174.
[33] L.A. Girifalco, Interaction potential for C60 molecules, J. Phys. Chem. 95 (1991) 5370–5371.
[34] L.A. Girifalco, Molecular-properties of C-60 in the gas and solid-phases, J. Phys. Chem. 96 (1992) 858–861.
[35] A. Jakalian, B. Bush, D. Jack, C. Bayly, Fast, efficient generation of high-quality atomic charges. AM1-BCC model: I. Method, J. Comput. Chem. 21 (2000) 132–146.
[36] A. Jakalian, D. Jack, C. Bayly, Fast, efficient generation of high-quality atomic charges. AM1-BCC model: II. Parameterization and validation, J. Comput. Chem. 23 (2002) 1623–1641.
[37] D.R. Roe, T.E. Cheatham III, PTRAJ and CPPTRAJ: Software for Processing and Analysis of Molecular Dynamics Trajectory Data", J. Chem. Theory Comput. 9 (2013) 3084–3095.
[38] N. Michaud-Agrawal, E.J. Denning, T.B. Woolf, O. Beckstein, MDanalysis: a toolkit for the analysis of molecular dynamics simulations, J. Compute. Chem. 32 (2011) 2319–2327.
[39] N. Choudhury, B. Pettitt, Dynamics of water trapped between hydrophobic solutes, J. Phys. Chem. B 109 (2005) 6422–6429.
[40] D. Boucher, J. Howell, Solubility characteristics of PCBM and C-60, J. Phys. Chem. B 120 (2016) 11556–11566.